THE JOURNAL OF PHYSICAL CHEMISTRY B

ARTICLE

pubs.acs.org/JPCB

Suppression and Regeneration of Camphor-Driven Marangoni Flow with the Addition of Sodium Dodecyl Sulfate

Yumihiko S. Ikura,[†] Ryoichi Tenno,[†] Hiroyuki Kitahata,[‡,§] Nobuhiko J. Suematsu,[∥,⊥] and Satoshi Nakata*[,†]

[†]Graduate School of Science, Hiroshima University, Kagamiyama 1-3-1, Higashi-Hiroshima 739-8526, Japan

[‡]Department of Physics, Graduate School of Science, Chiba University, 1-33, Yayoi-cho, Inage-ku, Chiba 263-8522, Japan

[§]PRESTO, JST, 4-1-8 Honcho, Kawaguchi, Saitama 332-0012, Japan

[∥]Graduate School of Advanced Mathematical Sciences, Meiji University, 1-1-1 Higashi-mita, Tama-ku, Kawasaki 214-8571, Japan

[⊥]Meiji Institute for Advanced Study of Mathematical Sciences (MIMS), 1-1-1 Higashi-mita, Tama-ku, Kawasaki 214-8571, Japan

Supporting Information

ABSTRACT: We investigated the Marangoni flow around a camphor disk on water with the addition of sodium dodecyl sulfate (SDS). The flow velocity decreased with an increase in the concentration of SDS in the aqueous phase, and flow was hardly observed around the critical micelle concentration (cmc), because SDS reduced the driving force of Marangoni flow. However, the flow velocity increased with a further increase in the concentration of SDS. Thus, the Marangoni flow is maximally inhibited around the cmc of SDS. In this paper, we concluded that the regeneration of Marangoni flow originates from an increase in the dissolution rate of camphor into the SDS aqueous solution.

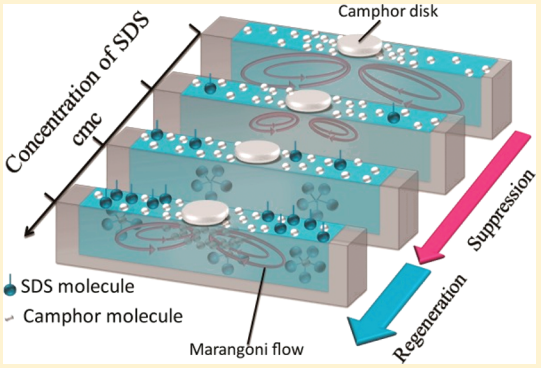

INTRODUCTION

Marangoni flow is a fascinating phenomenon observed at a gas/liquid or liquid/liquid interface,[1−3] as seen in the "tears of wine".[4−6] The driving force of Marangoni flow is the gradient of interfacial tension, which is induced by the heterogeneous distribution of temperature or the concentration of a substance at the interface. It has been reported that a surfactant generally suppresses Marangoni flow because the adsorption of the surfactant molecular layer at the interface causes quick smoothing of gradients of interfacial tension.[7,8] As another example of phenomena that result from Marangoni flow, "camphor dancing" has been well-known for several centuries,[9,10] and Marangoni flow is also observed around solid camphor on water.[11,12] Because the driving force of camphor motion is the gradient of the surface tension, Marangoni flow in a camphor−water system should also be suppressed by the addition of a surfactant.[12]

In this study, we investigated the effect of the addition of sodium dodecyl sulfate (SDS) to the aqueous phase on the intensity of Marangoni flow around a camphor disk. We found that the flow velocity decreased to almost zero, and then increased with an increase in the concentration of SDS. These different dependencies of the intensity of the Marangoni effect are discussed in relation to the surface tension of a mixed aqueous solution of SDS and camphor, and the dissolution rate of camphor in the SDS aqueous solution.

EXPERIMENTAL SECTION

Sodium dodecyl sulfate (SDS), D-glucose, and (+)-camphor were purchased from Sigma-Aldrich (St. Louis, Missouri, USA), Nacalai Tesque Inc. (Kyoto, Japan), and Wako Pure Chemicals (Kyoto, Japan), respectively. A camphor disk (diameter 3 mm, thickness 1 mm, mass 5 mg) was prepared using a pellet die set for Fourier transform infrared spectrometry (FTIR). For the aqueous phase, 2.3 mL of water with or without SDS (0−300 mM) was poured into a rectangular enclosure (width 5 mm, length 90 mm, water level 5 mm). Marangoni flow was monitored with a digital video camera (HDR-CX560V, SONY, Tokyo Japan; minimum time-resolution 1/30 s) in an air-conditioned room at 298 ± 2 K, and then analyzed by an image-processing system (ImageJ, National Institutes of Health, Gaithersburg, MD, USA). To observe convection in the aqueous phase, visualization particles (DIAION, HP20S, Mitsubishi Chemical Co., Tokyo, Japan; particle size 100−200 μm) were dispersed in the aqueous phase, the density of which was held constant at 1.1 g/mL by the addition of glucose. The surface tension was measured with a surface tensiometer (CBVP-A3, Kyowa Interface Science Co. Ltd., Saitama, Japan). We confirmed that the change in the surface tension with the addition of

Received: November 15, 2011
Revised: December 12, 2011
Published: December 14, 2011

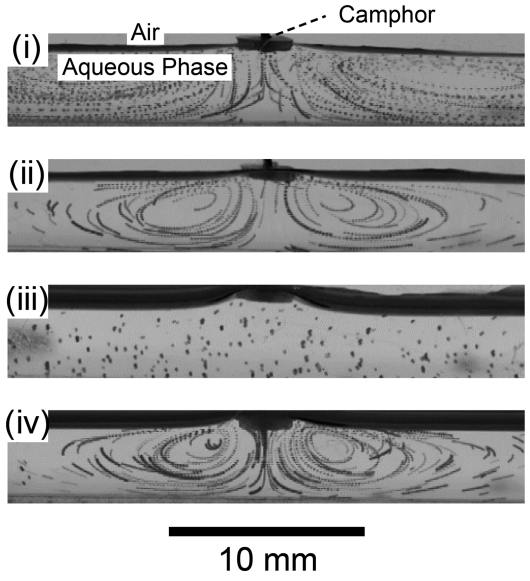

Figure 1. Experimental results for typical profiles of convective flow obtained by extracting the locations of visualization particles from a movie for different concentrations of SDS (C_{SDS} = (i) 0, (ii) 1, (iii) 7, and (iv) 300 mM). The exposure time of the superimposed image sequence was 1 s.

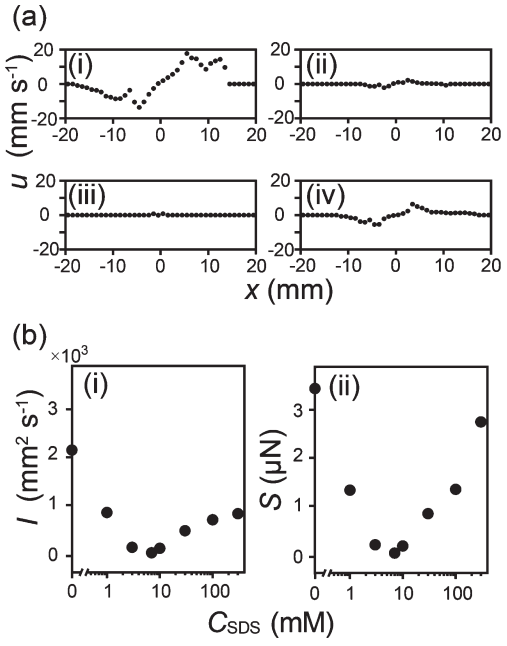

Figure 2. Experimental results for (a) the average horizontal velocity, $u(x)$, of particles at x with different concentrations of SDS (C_{SDS} = (i) 0, (ii) 1, (iii) 7, and (iv) 300 mM) and for (b) (i) I and (ii) S depending on C_{SDS} based on eqs 1, 2 respectively.

glucose was lower than 0.4 mN/m under the present conditions. The saturated concentration of camphor in the SDS aqueous solution was measured by UV/vis spectroscopy (UV-1800, Shimadzu, Kyoto, Japan). The saturated solution was prepared by stirring the SDS solution with excess camphor grains for 24 h and then filtering it.

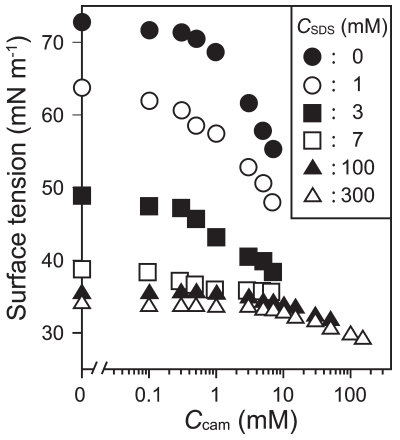

Figure 3. Experimental results for surface tension depending on the concentration of camphor mixed in the aqueous solutions with different concentrations of SDS (black circle, white circle, black square, white square, black triangle, and white triangle correspond to C_{SDS} = 0, 1, 3, 7, 100, and 300 mM, respectively).

RESULTS

When a camphor disk was fixed on an aqueous surface, the Marangoni flow was observed around the camphor disk. Figure 1 shows the trajectories of visualization particles for evaluating the features of Marangoni flow depending on the concentration of SDS (C_{SDS}) in the aqueous phase. Marangoni flow was observed at C_{SDS} = 0, 1, and 300 mM (Figure 1-i, 1-ii, and 1-iv) but was not clearly observed at C_{SDS} = 7 mM (Figure 1-iii). Figure 2a shows the horizontal flow velocity, $u(x)$, averaged over the surface layer to a depth of 0.5 mm depending on the horizontal position x at different C_{SDS}. Here, x = 0 corresponds to the position of the center of the camphor disk. By using the profiles in Figure 2a, we can extract the following two values to discuss the driving force of Marangoni effect: First, the intensity of the Marangoni flow, I, is obtained by the integration of $u(x)$ over the space:

$$I = \int_0^L u(x)\,dx \tag{1}$$

where L = 20 mm, because we confirm that the horizontal velocity at 20 mm from the camphor disk is almost zero. Next, to compensate for the change in viscosity due to the addition of the glucose, we calculate the intensity of the interfacial tension gradient, S, by considering that the flow velocity is proportional to the interfacial tension gradient divided by the viscosity:[11−13]

$$S = \eta I \tag{2}$$

where η is the viscosity. Figure 2b shows I and S for different C_{SDS}. With an increase in C_{SDS}, I and S clearly decreased to almost zero at C_{SDS} < 7 mM, but gradually increased at C_{SDS} > 7 mM.

To clarify the origin of the driving force, the following three parameters were measured for various SDS concentrations: (i) surface tension, (ii) saturated concentration of camphor, and (iii) dissolution rate of camphor molecules from the disk (k_{dis}). As shown in Figure 3, the surface tension γ clearly decreased with an increase in the camphor concentration (C_{cam}). Especially, the slope of the surface tension isotherm, $|\partial\gamma/\partial C_{cam}|$, at a high concentration region of C_{cam} decreased with an increase in C_{SDS}. Here, the measurement range of C_{cam} depended on C_{SDS}, because saturated C_{cam} increased with an increase in C_{SDS} (Figure S1, Supporting Information).

dx.doi.org/10.1021/jp210990a |J. Phys. Chem. B 2012, 116, 992–996

The dissolution rate, k_{dis}, was obtained by measuring the time series of the volume of a camphor disk ($V(t)$) depending on C_{SDS}, as indicated in Figure 4a. Here, $V(t)$ was obtained by measuring the basal area of the camphor disk with the assumption of a constant aspect ratio. As seen in Figure 4a, $V(t)$ exponentially decreased with time. Thus, we can calculate the dissolution rate, k_{dis}, by fitting the following equation:

$$V(t) = V_0 \exp(-k_{dis}t) \tag{3}$$

where V_0 is the initial volume of the camphor disk (7.1 mm^3). At $C_{SDS} < 7$ mM, k_{dis} hardly changed. In contrast, at $C_{SDS} > 7$ mM, k_{dis} increased with an increase in C_{SDS}, as shown in Figure 4b.

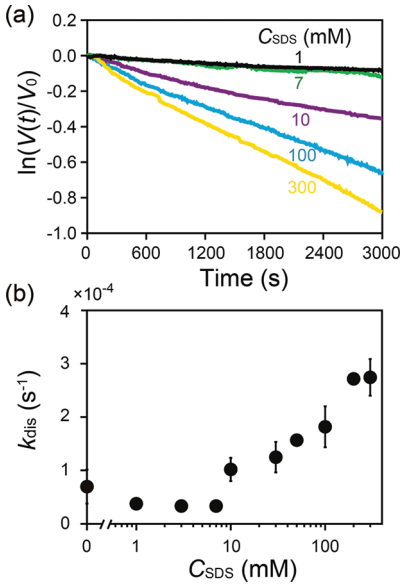

Figure 4. Experimental results for (a) the time-course of the relative change in the volume of a camphor disk, $\ln(V(t)/V_0)$, and (b) the dissolution rate, k_{dis}, of camphor into the aqueous solutions with different concentrations of SDS.

NUMERICAL CALCULATIONS

To qualitatively reproduce the experimental results, and to elucidate the mechanism of the suppression and regeneration of Marangoni flow, we introduce a mathematical model for the system. We consider the flow velocity in the two-dimensional region which consists of the vertical (y-axis) and horizontal (x-axis) directions. The incompressibility of the medium is described as

$$\nabla \cdot \boldsymbol{v} = 0 \tag{4}$$

The Navier−Stokes equation is written as[11,13−19]

$$\rho\left(\frac{\partial v}{\partial t} + \boldsymbol{v}\cdot\nabla\boldsymbol{v}\right) = \eta\nabla^2\boldsymbol{v} - \nabla p \tag{5}$$

where ρ is the density of the aqueous solution, $\boldsymbol{v}(t,\boldsymbol{x}) = (v_x(t,\boldsymbol{x}), v_y(t,\boldsymbol{x}))$ is the flow velocity, and $p(t,\boldsymbol{x})$ is the pressure. Here, Cartesian coordinates are set so that the surface is parallel to the x-axis, and y is the height from the bottom of the region. $x = 0$ is the center of the camphor disk. We take the following boundary condition to consider the effect of the surface tension:

$$\begin{cases} \left.\dfrac{\partial v_x}{\partial y}\right|_{y=L_y} = \dfrac{1}{\eta}\dfrac{\partial \gamma}{\partial x} \\ v_y(t,(x,L_y)) = 0 \end{cases} \tag{6}$$

and fixed boundary conditions at the sides and bottom of the region:

$$v_x(t,\boldsymbol{x}) = v_y(t,\boldsymbol{x}) = 0 \tag{7}$$

where L_y is the water depth. The relationship between the surface tension and the surface concentration of the camphor layer (c), which depends on C_{SDS}, was qualitatively reproduced by a sigmoid function. So, we adopted the following equation:[11,20,21]

$$\gamma(c) = \frac{\gamma_0 a^n}{a^n + c^n} + \gamma_1 \tag{8}$$

where the values of γ_0, γ_1, and a are determined for each C_{SDS} by fitting the experimental results in Figure 3, and n is a positive

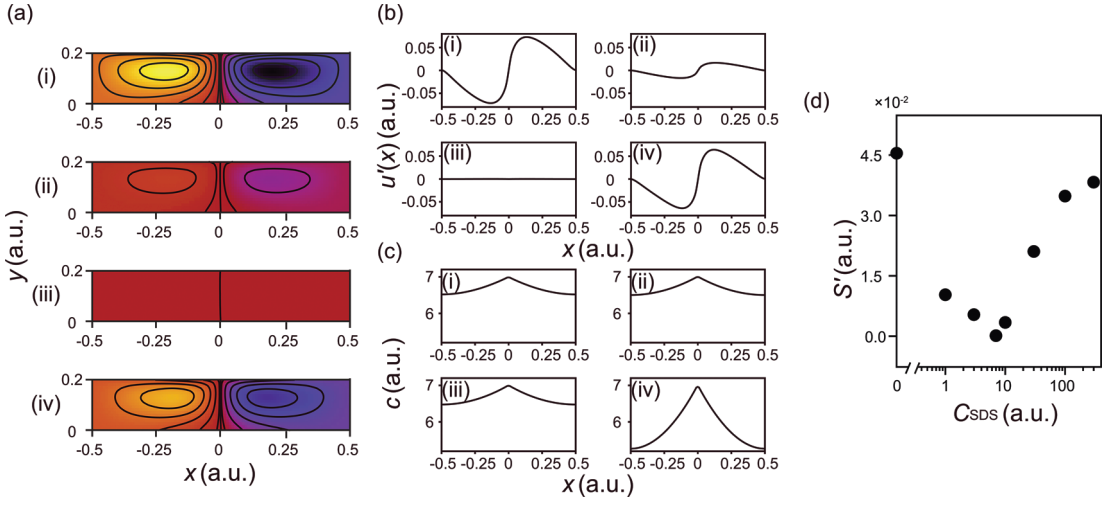

Figure 5. Numerical results for convective flow based on eqs 4−13. (a) Streamlines with different concentrations of SDS (C_{SDS} = (i) 0, (ii) 1, (iii) 7, and (iv) 300), where dark (blue) and bright (red) colors correspond to clockwise and counterclockwise flow, respectively. (b) The velocity of flow at the surface $u'(x)$ with different C_{SDS}(= (i) 0, (ii) 1, (iii) 7, and (iv) 300). (c) Camphor layer, c, depending on the position x with different C_{SDS} (= (i) 0, (ii) 1, (iii) 7, and (iv) 300), and (d) S' depending on C_{SDS}. The parameters used were $n = 2$, $L_x = 0.5$, $L_y = 0.2$, $\rho = 1$, $\eta = 0.5$, $D = 0.1$, $k_1 = 0.01$, $k_3 = 1000$, and $c_0 = 7$. (γ_0, γ_1, a, k_2) is (18, 53.6, 2.59, 0.0625) for $C_{SDS} = 0$, (12.7, 49.3, 1.29, 0.0626) for $C_{SDS} = 1$, (2.96, 35.8, 0.3, 0.0643) for $C_{SDS} = 7$, and (3.12, 30.7, 15.1, 0.268) for $C_{SDS} = 300$, respectively.

dx.doi.org/10.1021/jp210990a |J. Phys. Chem. B 2012, 116, 992–996

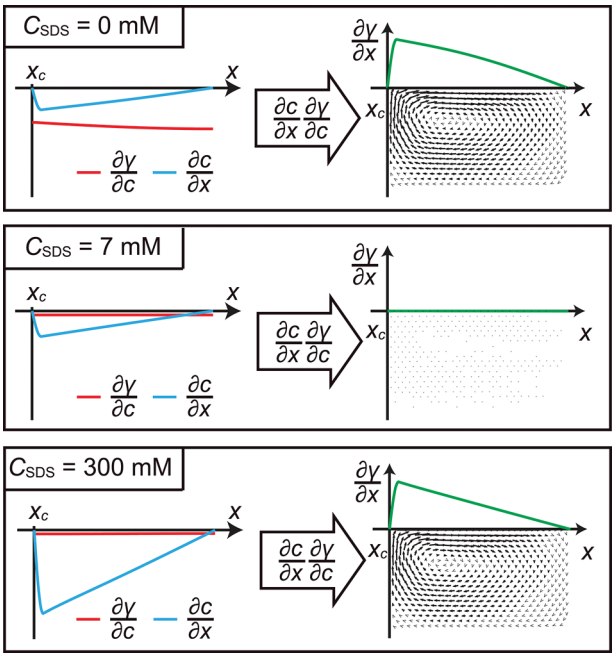

Figure 6. Schematic illustration of the mechanism of Marangoni flow depending on C_{SDS}. $\partial\gamma/\partial c$ and $\partial c/\partial x$ in the radial direction are shown on the left, and their product, $\partial\gamma/\partial x$, is shown on the right.

integer, where we use $n = 2$ for sake of simplicity. Now, we suppose that the concentration of the camphor molecules in air and bulk is ignorable because the experimental system is an open system, that the diffusion of the camphor molecules is fast enough, and that the volume of the water chamber is significantly larger than that of the camphor disk. Hence, we should consider only the sublimation to the air and dissolution to the bulk, not the adsorption from the air or the bulk, for the time change in the surface concentration of the camphor layer, $c(t,x)$. On the basis of previous papers,[21,22] $c(t,x)$ can be described by the following reaction−diffusion−advection equation:

$$\frac{\partial c}{\partial t} + (\boldsymbol{v}\cdot\nabla)c = D\nabla^2 c - (k_1 + k_2(C_{SDS}))c + F(c,x;r) \quad (9)$$

where k_1 is the sublimation rate, $k_2(C_{SDS})$ is the dissolution rate for each C_{SDS}, D is the diffusion constant of camphor molecules at the interface, and r is the radius of the camphor disk. $F(c,x;r)$ corresponds to the development of camphor molecules from the camphor disk to the surface:

$$F(c,x;r) = \begin{cases} k_3(c_0 - c) & |x| \le r \\ 0 & |x| > r \end{cases} \quad (10)$$

where k_3 is the rate of development of the camphor layer from the camphor disk and c_0 is the saturated surface concentration of it. For the concentration of the camphor layer at the boundary of the water surface, we used the Neumann boundary condition:

$$\frac{\partial c}{\partial x} = 0 \text{ at } x = -L_x, L_x \quad (11)$$

where $2L_x$ is the horizontal length of the region.

Using eqs 4−11, we performed numerical calculations while varying C_{SDS}. Figure 5 shows the results of the numerical calculations for (a) streamlines, (b) the velocity of flow at the surface ($u'(x)$), (c) the spatial distribution of the surface concentration of the camphor layer, and (d) the intensity of the Marangoni effect (S'). Here, we defined $u'(x)$ as

$$u'(x) = \lim_{t\to\infty} v_x(t,(x,L_y)) \quad (12)$$

which corresponds to $u(x)$ in the experiment, and S' as

$$S' = \int_0^{L_x} u'(x)\,dx \quad (13)$$

which corresponds to S in eq 2 with different C_{SDS}. Although the numerical calculation was partially based on the fitting of experimental data, the results of Figure 5 indicated the cause of the regeneration of Marangoni flow.

DISCUSSION

We now discuss the velocity of Marangoni flow depending on the concentration of SDS (C_{SDS}). I and S depend on the velocity of Marangoni flow, and the local gradient of surface tension becomes the driving force of Marangoni flow. Therefore, we consider the surface tension gradient around the camphor disk, $\partial\gamma/\partial x$, to clarify the mechanism of change in the velocity of Marangoni flow. The relationship between the surface tension and the surface concentration of camphor can be described as

$$\frac{\partial \gamma}{\partial x} = \frac{\partial \gamma}{\partial c}\frac{\partial c}{\partial x} \quad (14)$$

On the basis of the experimental and numerical results, we propose a mechanism for the generation of Marangoni flow in a camphor−SDS system by considering three concentration regions (C_{SDS} < 7 mM, C_{SDS} ∼ 7 mM, and C_{SDS} > 7 mM), as shown in Figure 6.

$|\partial\gamma/\partial c|$ at C_{SDS} < 7 mM is clearly larger than those in the other concentration regions. On the other hand, the dissolution rate, k_{dis}, is clearly smaller than those in the other concentration regions, as shown in Figure 4a, b. These results suggest that the camphor distribution is also slightly changed in this concentration range of SDS; i.e., $\partial c/\partial x$ around the camphor disk is almost constant despite the difference in C_{SDS}.

However, the velocity $u(x)$ and the intensity of the Marangoni effect S clearly decrease to almost zero with an increase in C_{SDS} up to ∼7 mM, as shown in Figure 2a, b. Figure 3 also suggests that $|\partial\gamma/\partial c|$ decreases with an increase in C_{SDS} and becomes very small at C_{SDS} ∼ 7 mM. S decreases with an increase in C_{SDS}, because the driving force $|\partial\gamma/\partial x|$ decreases in proportion to $|\partial\gamma/\partial c|$, because $|\partial\gamma/\partial c|$ is almost constant at a location as indicated in eq 14. Because both $|\partial\gamma/\partial c|$ and $|\partial\gamma/\partial x|$ are very small, the driving force becomes minimum, and therefore the minimum value of S is observed at C_{SDS} ∼ 7 mM.

For C_{SDS} > 7 mM, $u(x)$ and S increase with an increase in C_{SDS}, as shown in Figure 2a and 2b-ii. According to eq 14, Marangoni flow is not clearly observed in this concentration range because $|\partial\gamma/\partial c|$ is small (Figure 3). However, the magnitude of Marangoni flow actually increases with an increase in C_{SDS}. We consider this question in relation to the dissolution rate of camphor into a SDS solution. The dissolution rate of camphor into the SDS solution drastically increases above the critical micelle concentration (cmc). Thus, the camphor layer rapidly dissolves into the aqueous solution once it develops to the surface from the camphor disk. Therefore, we can speculate that the density distribution of the camphor layer becomes steep

dx.doi.org/10.1021/jp210990a |J. Phys. Chem. B 2012, 116, 992–996

around the camphor disk; i.e., $|\partial c/\partial x|$ in eq 14 becomes large. The results of the numerical calculation in Figure 5c support the above speculation. Thus, the driving force $|\partial\gamma/\partial x|$ is large enough to generate the flow around the camphor disk, because $|\partial c/\partial x|$ is large enough even if $|\partial\gamma/\partial c|$ is small.

CONCLUSIONS

In this study, the suppression and regeneration of Marangoni flow around a camphor disk were observed under the conditions around the cmc of SDS in an aqueous phase. On the basis of the experimental and numerical results, we analyzed this suppression and regeneration of Marangoni flow in relation to the dissolution rate of camphor into the SDS aqueous solution, and the dependency of surface tension on the camphor in the SDS aqueous solution. In other words, the suppression and regeneration was suggested to be a nonlinear driving force that can be described as $\partial\gamma/\partial x = (\partial\gamma/\partial c)(\partial c/\partial x)$. When the concentration of SDS in the aqueous solution was lower than the cmc, the flow was suppressed by a decrease in $|\partial\gamma/\partial c|$ that accompanied the increase in the concentration of SDS. However, when the concentration of SDS in the aqueous solution was larger than the cmc, the flow was regenerated because $|\partial c/\partial x|$ became large enough due to an increase in the dissolution rate of camphor into the SDS aqueous solution. As for discussion on the micelle of SDS and camphor molecules at the molecular level, a spectroscopic method should be done. We confirmed that a chemical shift of ^{13}C NMR for camphor dissolved in a SDS aqueous solution was changed depending on their concentrations (data not shown). We will report the experimental results separately in the near future.

We have previously reported that a camphor disk located at the surface of an aqueous phase exhibited different types of motion depending on the kinds of surfactants.[23] This dependency of the Marangoni effect on the kinds of surfactants still requires further investigation. The dependency of the Marangoni effect on the shape and size of the chamber and the effect of camphor molecules on the cmc value for SDS should also be examined in future studies.

ASSOCIATED CONTENT

Supporting Information. Description of the saturated concentration of camphor in a SDS aqueous solution. This material is available free of charge via the Internet at http://pubs.acs.org.

AUTHOR INFORMATION

Corresponding Author
*Tel & fax: +81-82-424-7409. E-mail: nakatas@hiroshima-u.ac.jp.

ACKNOWLEDGMENT

We thank Professor Masaharu Nagayama (Kanazawa University, Japan) for his helpful discussion regarding the mechanism of the camphor system, and Mr. Yui Matsuda and Mr. Makoto Yashima for their technical support. This work was supported in part by a Grant-in-Aid for Scientific Research (No. 23111715), and a Grant-in-Aid for the Global COE Program "Formation and Development of Mathematical Sciences Based on Modeling and Analysis".

REFERENCES

(1) Scriven, L. E.; Sternling, C. V. *Nature* **1960**, *187*, 186–188.
(2) Bekki, S.; Vignes-Alder, M.; Nakache, E.; Adler, P. M. *J. Colloid Interface Sci.* **1990**, *140*, 492–506.
(3) de Gennes, P. G.; Brochard-Wyart, F.; Quéré, D. *Capillarity and Wetting Phenomena: Drops, Bubbles, Pearls, Waves*; Springer: New York, 2004.
(4) Fournier, J. B.; Cazabat, A. M. *Europhys. Lett.* **1992**, *20*, 517–522.
(5) Thomson, J. *Philos. Mag.* **1855**, *10*, 330–333.
(6) Vuilleumier, R.; Ego, V.; Neltner, L.; Cazabat, A. M. *Langmuir* **1995**, *11*, 4117–4121.
(7) Lewisa, J. B.; Pratt, H. R. C. *Nature* **1953**, *171*, 1155–1156.
(8) Garner, F. H.; Nutt, C. W.; Moutadi, M. F. *Nature* **1955**, *175*, 603–605.
(9) Tomlinson, C. *Proc. R. Soc. London* **1860**, *11*, 575–577.
(10) Rayleigh, L. *Proc. R. Soc. London* **1890**, *47*, 364–367.
(11) Kitahata, H.; Hiromatsu, S.; Doi, Y.; Nakata, S.; Islam, M. R. *Phys. Chem. Chem. Phys.* **2004**, *6*, 2409–2414.
(12) (a) Kitahata, H.; Kawata, K.; Takahashi, S.; Nakamura, M.; Sumino, Y.; Nakata, S. *J. Colloid Interface Sci.* **2010**, *351*, 299–303. (b) Kitahata, H.; Kawata, K.; Sumino, Y.; Nakata, S. *Chem. Phys. Lett.* **2008**, *457*, 254–258.
(13) Linde, H.; Schwartz, P.; Wilke, H. In *Dynamics and Instability of Fluid Interfaces*; Sørensen, T. S., Ed.; Springer-Verlag: Berlin, 1979.
(14) Grigorieva, O. V.; Kovalchuk, N. M.; Grigoriev, D. O.; Vollhardt, D. *J. Colloid Interface Sci.* **2003**, *261*, 490–497.
(15) Kitahata, H.; Aihara, R.; Magome, N.; Yoshikawa, K. *J. Chem. Phys.* **2002**, *116*, 5666–5672.
(16) Rongy, L.; de Wit, A. *Phys. Rev. E* **2008**, *77*, 046310.
(17) Miike, H.; Miura, K.; Nomura, A.; Sakurai, T. *Physica D* **2009**, *239*, 808–818.
(18) Landau, L. D.; Lifshits, E. M. *Fluid Mechanics*, 2nd ed.; Pergamon Press: London, 1987.
(19) Kovalchuk, V. I.; Kamusewitz, H.; Volhardt, D.; Kovalchuk, N. M. *Phys. Rev. E* **1999**, *60*, 2029–2036.
(20) Nakata, S.; Iguchi, Y.; Ose, S.; Kuboyama, M.; Ishii, T.; Yoshikawa, K. *Langmuir* **1997**, *13*, 4454–4458.
(21) Nagayama, M.; Yadome, M.; Murakami, M.; Kato, N.; Kirisaka, J.; Nakata, S. *Phys. Chem. Chem. Phys.* **2009**, *11*, 1085–1090.
(22) Hayashima, Y.; Nagayama, M.; Doi, Y.; Nakata, S.; Kimura, M.; Iida, M. *Phys. Chem. Chem. Phys.* **2002**, *4*, 1386–1392.
(23) Nakata, S.; Murakami, M. *Langmuir* **2010**, *26*, 2414–2417.

NOTE ADDED AFTER ASAP PUBLICATION

This paper was published on the Web on January 6, 2012. An addition was made to reference 12. The corrected version was reposted on January 11, 2012.